Ultrafast non-local control of spontaneous emission

LETTERS
PUBLISHED ONLINE: 14 SEPTEMBER 2014 | DOI: 10.1038/NNANO.2014.190
nature nanotechnology

Ultrafast non-local control of spontaneous emission

Chao-Yuan Jin[1]*, Robert Johne[1,2], Milo Y. Swinkels[1], Thang B. Hoang[1†], Leonardo Midolo[1†], Peter J. van Veldhoven[1] and Andrea Fiore[1]

The radiative interaction of solid-state emitters with cavity fields is the basis of semiconductor microcavity lasers and cavity quantum electrodynamics (CQED) systems[1]. Its control in real time would open new avenues for the generation of non-classical light states, the control of entanglement and the modulation of lasers. However, unlike atomic CQED or circuit quantum electrodynamics[2–6], the real-time control of radiative processes has not yet been achieved in semiconductors because of the ultrafast timescales involved. Here we propose an ultrafast non-local moulding of the vacuum field in a coupled-cavity system as an approach to the control of radiative processes and demonstrate the dynamic control of the spontaneous emission (SE) of quantum dots (QDs) in a photonic crystal (PhC) cavity on a ~200 ps timescale, much faster than their natural SE lifetimes.

When a two-level emitter in the excited state interacts with the vacuum field of a cavity mode, the evolution of the system is determined by the interplay of the coupling rate g, interaction time T and cavity-loss rate κ. The control of one or more of these parameters in real time allows optimizing the interaction for the desired application, resulting, for example, in entangled emitter–photon states[2], or in single-photon states with an optimized waveform for quantum networking applications[3]. In atomic CQED systems, the control of the radiative interaction is realized at microwave frequencies by varying the interaction time T in the range of tens of microseconds[2], and at optical frequencies by adiabatic passage techniques[3–5], which effectively allow the shaping of the coupling rate g on timescales of 100 ns. In superconducting circuit quantum electrodynamics, the cavity-loss rate κ has been changed on a timescale of 100 ns by the electrical control of circuit elements[6]. However, in semiconductor systems based, for example, on QDs in PhC cavities, these approaches are difficult to implement because of the different energy-level structures and the faster cavity loss and emitter decoherence rate (typically subnanoseconds). The ideal control method for semiconductor nanocavities would allow the ultrafast manipulation of the coupling rate g and/or of the cavity-loss rate κ, without directly affecting the population and the phase of the emitter. Although various methods for the control of semiconductor CQED systems have been demonstrated, for example by tuning the emitter or cavity frequency using electric field[7], strain[8] or nanomechanical deformation[9,10], none of these has been shown to provide the control of radiative processes on the required subnanosecond timescales. The fast wavelength-detuning techniques theoretically proposed in Johnson *et al.*[11] and Thyrrestrup *et al.*[12] are extremely challenging to implement without directly perturbing the emitter's evolution, and are intrinsically associated with a wavelength chirp. Here we propose an approach that enables the non-local and ultrafast control of the coupling rate and/or the cavity-loss rate in a solid-state system. We show its implementation in semiconductor QDs weakly coupled to a PhC coupled-cavity system, which demonstrates, for the first time, the ultrafast control of SE dynamics at optical frequencies with a temporal resolution of about 200 ps, which can be reduced further to the few picoseconds range.

Our approach is based on ultrafast moulding of the vacuum field, and thereby the coupling rate and cavity loss, seen by a dipole emitter sitting in a 'target' cavity, by changing the resonant wavelength of an adjacent Fabry–Pérot (FP) cavity coupled to the target cavity through a semitransparent mirror (Fig. 1a). When the two cavities are out of resonance, the modes of the system are approximated well by the modes of uncoupled cavities, where, by design, the periodic FP modes have a lower quality factor (Q factor) compared with the mode of the target cavity. A change in the refractive index of the FP cavity produces a spectral shift of the FP modes and brings one of them into resonance with the

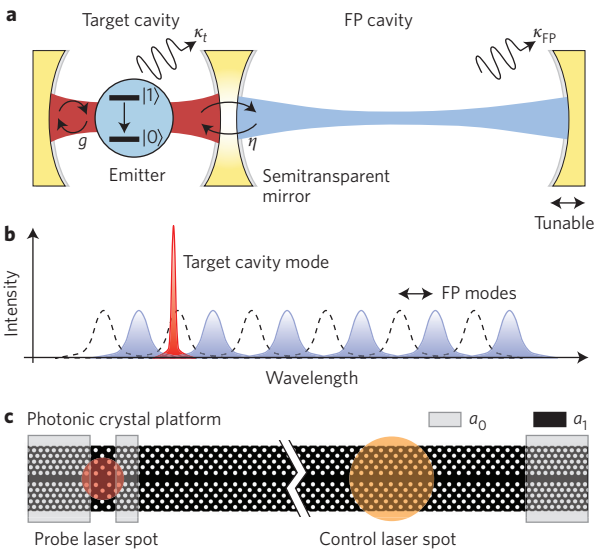

Figure 1 | Scheme of the non-local control of the emitter–cavity interaction. a, Two cavities with different Q factors and mode volumes are coupled through a semi-transparent mirror. **b**, Bringing one of the FP cavity modes into the resonance of the target cavity mode produces a redistribution of the mode field and a change of Q factor. **c**, A schematic image of coupled PhC cavities. The probe laser beam is located at the target cavity to generate the μPL signal and the control laser beam is focused on the FP cavity, at 30 μm distance from the target cavity.

[1]COBRA Research Institute, Eindhoven University of Technology, P.O. Box 513, NL-5600MB Eindhoven, The Netherlands, [2]Max Planck Institute for the Physics of Complex Systems, Nöthnitzer Str. 38, 01187 Dresden, Germany, †Present addresses: Department of Physics, Duke University, North Carolina 27708, USA (T.B.H.), Niels Bohr Institute, University of Copenhagen, Copenhagen, 2100 Denmark (L.M.). *e-mail: c.jin@tue.nl

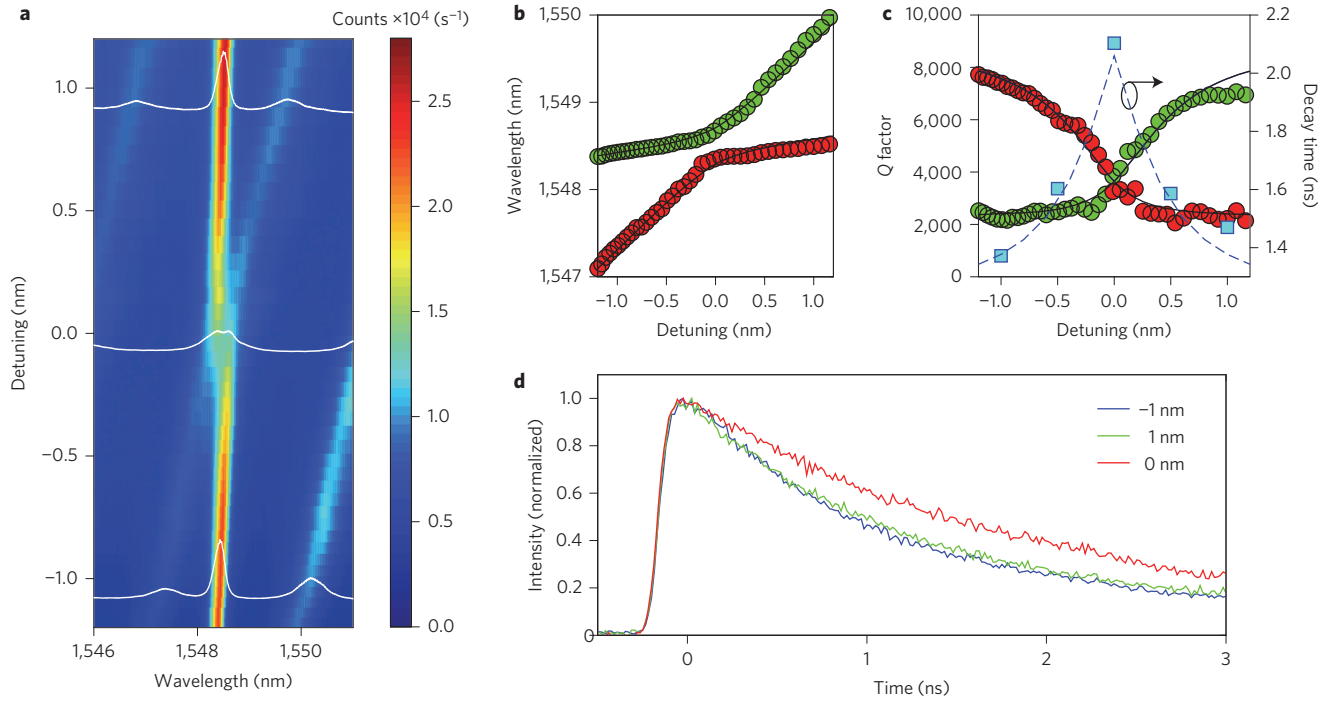

Figure 2 | Quasi-static modulation of the *Q* factor and SE rate. a, A μPL map exhibits the target cavity mode and FP modes at different detunings, which correspond to different CW laser powers on the FP cavity. The three white curves are the μPL spectra at detunings of –1.0, 0 and 1.0 nm. **b**, The wavelengths of the coupled modes as functions of the detuning. The black curves are fits using the coupled-mode theory. The observed anticrossing shows that the two cavities are at the edge between the strong and weak coupling regimes. **c**, The *Q* factors of coupled modes (green and red circles) and the SE decay times (blue squares) as functions of the detuning. The black lines are the fitted values using the coupled-mode theory and the blue dashed line shows the decay times calculated by using the Master equation model. **d**, The SE decay curves at detunings of –1.0, 0 and 1.0 nm, which correspond to the white spectra in **a**.

target cavity mode (Fig. 1b). This causes a redistribution of the vacuum field seen by the emitter, with a corresponding increase in the effective mode volume and reduction of the *Q* factor, and thereby changes the emitter-field coupling rate and the loss rate. If the change of the FP spectrum is produced by an ultrafast laser pulse from the photoexcitation of free carriers[13,14], the vacuum field responds within a timescale set by the target–FP coupling rate (typically picoseconds) and the emitter experiences a dynamic modulation of the local density of states (LDOS) during its interaction with the cavity. As the free carriers are injected distant from the target cavity (that is, the control is 'non-local'), they do not directly perturb the population and phase coherence of the emitter. A simple analysis based on coupled-mode theory (see Methods and Supplementary Methods) shows that the emitter interacts with the coupled mode with a rate $g_1 = \alpha g$, where α is the target-cavity component of the electric field of the coupled mode, and g is the interaction rate between the emitter and the uncoupled target cavity. Although this g modulation is generally applicable to any radiative interaction, we focus here on the modulation of the SE rate of emitters weakly coupled to a cavity to give a first experimental demonstration of the concept. The SE rate γ_1 into one of the coupled modes, normalized by that in the uncoupled target cavity γ_t, is given by:

$$\frac{\gamma_1}{\gamma_t} \cong \left|\frac{g_1}{g}\right|^2 \frac{\kappa_t}{\kappa_1} = |\alpha|^2 \frac{Q_1}{Q_t}$$

where $Q_1(\kappa_1)$ and $Q_t(\kappa_t)$ are the *Q* factors (loss rates) of the coupled mode and uncoupled target cavity, respectively. The SE rate is affected both by the change in the coupling rate g (term $|\alpha|^2$) and loss rate κ, which are controlled by the target-FP detuning. Also, a pure g modulation is possible by choosing the *Q* factor of the FP cavity equal to that of the target cavity.

We implemented this concept using PhC cavities and QDs as emitters. Coupled PhC cavities were investigated previously as examples of photonic molecules[15–17], for *Q*-factor tuning[13,14,18] and coupled CQED[19]. Two double-heterostructure cavities[20] are defined by slightly modifying the lattice constant along a W1 PhC waveguide from a_0 to $a_1 = 1.03 \times a_0$ (Fig. 1c). In the first series of experiments, the change in the SE rate of QDs in the target cavity was characterized in quasi-static conditions by thermo-optic tuning of the FP cavity. The FP modes shift to longer wavelengths because of heating when the excitation power increases[21], which changes the detuning between two cavities (Fig. 2a). When the central FP mode anticrosses the target cavity mode, a decrease in emission intensity is observed and the *Q* factor decreases by a maximum factor of 2.0 (Fig. 2a–c). Depending on the detuning, the cavity wavelength and the *Q* factor can be fitted well by the coupled-mode theory (Fig. 2b,c). The microphotoluminescence (μPL) decay times strongly depend on the detuning (Fig. 2c,d) and are reproduced well by the Master equation model, taking into account the homogeneous broadening at the measurement temperature of 77 K, estimated as 250 μeV (see the Supplementary Information). After deducting the measured effect of emission into the leaky modes of the PhC, a change in the SE rate in the cavity mode by a factor of 2.7 is derived, which is attributed partly to the relative change in the effective *Q* (by a factor of ~1.34, see the Supplementary Information) and partly to the redistribution of the vacuum field term $|\alpha|^2$ (by a factor of ~2).

In a second set of experiments, the dynamic control of SE was achieved by replacing the thermo-optic tuning with free-carrier injection. In this case, a pulsed laser injects free carriers into the FP cavity. When the initial detuning between the target and FP

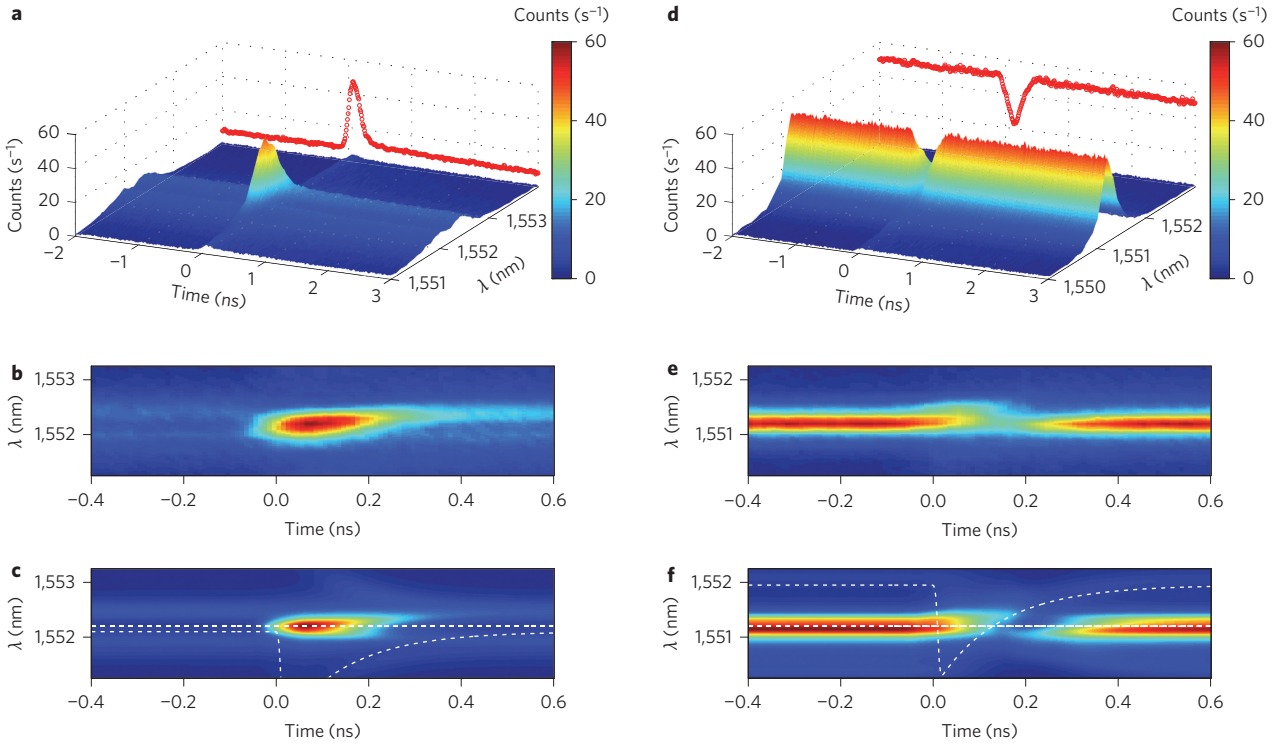

Figure 3 | Dynamic control of SE at the target cavity. a, A time-resolved μPL map, for an initial detuning of 0 nm, made by measuring the decay curves at different wavelengths. The target cavity is excited with a CW laser source when the pulse excitation at the FP cavity brings the FP mode out of resonance. The curve at the backplane is the measured time-resolved μPL trace at a wavelength of 1,552.2 nm. **b**, Top view of the map in **a**. **c**, The simulation results compared to **b**. The uncoupled wavelengths of the target and FP modes are shown by the white dotted curves. **d–f**, The same as **a–c** for an initial detuning of 0.6 nm. The curve at the backplane is the measured time-resolved μPL trace at a wavelength of 1,551.2 nm.

cavity is adjusted to 0 nm, two coupled modes are observed at 1,552.0 and 1,552.4 nm. The laser pulse produces a blue shift of the FP mode, which brings it out of resonance with the target cavity, and the SE rate from QDs in the target cavity is enhanced because of the increase in the Q factor and the increased localization of the vacuum field (Fig. 3a–c). This gives rise to a peak at time zero in the three-dimensional map, which lasts until the FP mode relaxes to the initial wavelength through diffusion and the recombination of free carriers. The duration of this pulse of SE (232 ps at full-width half-maximum (FWHM)) is related to the free-carrier lifetime in the FP cavity, and not to the emitter's lifetime—this shows the possibility of modulating SE at frequencies of several gigahertz, well above the bandwidth limitation related to the lifetime. This dynamic process is simulated by a Master equation model (see the Supplementary Information), which includes the effect of pumping by several QDs via their homogeneous broadening and reproduces the PL temporal dependence very well (Fig. 3c). The observed modulation depth at the peak, $I_{max}/I_0 = 3.3$, results from the combined effect of the LDOS enhancement, the increase of photon population caused by the Q change and the change in the collection efficiency as a result of the redistribution of the vacuum field.

For the opposite situation of non-zero detuning, the FP and target cavity modes can be transiently brought into resonance (Fig. 3d–f). This produces a sharp dip (246 ps FWHM) in the SE intensity because of the LDOS reduction caused by the vacuum field delocalization and Q-factor decrease, which confirms that the peak in Fig. 3a is not a result of the additional PL produced by the injected carriers. For this case, the measured peak modulation depth is $I_0/I_{min} = 2.0$. Here the modulation occurs over the entire mode spectrum, and clearly differs from the static modulation of the SE rate using PhC cavities[22] and the dynamic modulation, which may, in principle, be obtained by changing the emitter–cavity detuning with ultrafast control of the cavity wavelength[11,12,23] or by Stark tuning of the exciton energy[8]. Indeed, our method directly changes the SE rate by controlling the interaction term g and loss rate κ. This allows the chirp of the emitted photons to be minimized. This chirp reduces the coupling efficiency to another cavity and is therefore detrimental to application in quantum-information processing[24].

To demonstrate further the flexibility of our approach, we show the control of the temporal SE decay profile of the emitters in the target cavity. In this case, both the target and the FP cavity are pumped by the same pulsed laser, with variable delay. The excitation power at the target cavity produces an initial blue shift in the target cavity mode (as seen in the inset of Fig. 4a) caused by free-carrier injection. To avoid the effect of this blue shift we choose delays such that the target cavity wavelength is stabilized. When the initial detuning is zero and the pulse exciting at the FP cavity is delayed by 2.0 ns, a spike is observed in the PL signal collected from the target cavity when the FP mode is brought out of resonance. The timing of the spike can be controlled by the delay, as shown in Fig. 4a for delays of 1.5, 2.0 and 2.5 ns. For the opposite situation in which the static detuning between coupled modes is set to 0.6 nm, the FP mode is transiently brought into resonance so that the expected dip appears (Fig. 4b).

In our demonstration, the temporal resolution is determined by the free-carrier lifetime, which potentially can be reduced down to a few picoseconds by applying an electric field in the control cavity[25]. This would allow shaping of the control-cavity frequency and thereby the LDOS at the target cavity on picosecond timescales by the simple control of the pump–pulse temporal profile.

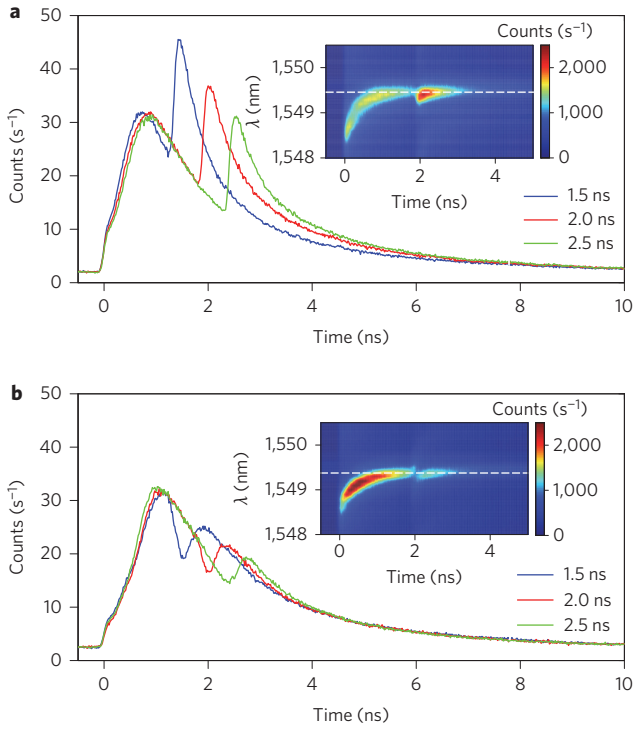

Figure 4 | Dynamic modulation of the SE decay curves at the target cavity. **a**, μPL decay curves at the wavelength indicated by a white dashed line in the inset, with different delay times of 1.5, 2.0, 2.5 ns of the control pulse. The inset shows a time-resolved μPL map at zero initial detuning. **b**, The same as **a** for an initial detuning of −0.6 nm.

In the context of CQED, this ultrafast non-local control can be used to engineer the shape of single-photon pulses and for the on–off switching of Rabi oscillations, without directly disturbing the carrier population in the target cavity. Although, for simplicity, the experiments presented here were performed with an ensemble of QDs, the extension to the single-QD/single-photon case is straightforward, as single QDs are easily coupled to PhC cavity modes[1]. Although our initial demonstration focused on the control of SE, the mode field also determines the stimulated emission rate. Our method of ultrafast moulding of the vacuum field can therefore be used to change dynamically the Q factor and/or the gain in lasers. The ultrafast Q-factor tuning directly affects the laser output via the cavity-loss term, and it opens the way to Q-switching in nanocavity lasers[26]. The modulation of the cavity field, however, changes the modal gain via the confinement factor, and represents a new type of gain switching that does not rely on directly altering the carrier population via current injection.

Methods

Coupled-mode theory. The system of three coupled oscillators (the emitter, the target and FP cavities) can be described by a non-Hermitian Hamiltonian[27]:

$$\mathrm{H} = \hbar \begin{bmatrix} \omega_0 & g & 0 \\ g & \omega_t - i\kappa_t & \eta \\ 0 & \eta & \omega_{FP} - i\kappa_{FP} \end{bmatrix}$$

where ω_0, ω_t and ω_{FP} are the angular frequencies of the emitter, the uncoupled target and the FP cavity modes, respectively, and κ_t and κ_{FP} are the corresponding loss rates. We assume that the emitter couples only to the target cavity with an interaction strength g, where we fix the interaction to the weak coupling regime $g \ll \kappa_t, \kappa_{FP}$. The coupling rate between the two cavities is η. By diagonalizing the 2×2 submatrix of the cavities, the normalized mode functions $E_{1,2}(r)$ of the coupled modes are calculated on the basis of the isolated cavity modes $E_t(r)$ and $E_{FP}(r)$, $E_{1,2}(r) = \alpha_{1,2}E_t(r) + \beta_{1,2}E_{FP}(r)$ with $\alpha_1 = \beta_2 = \alpha$, and $\alpha_2 = -\beta_1 = \beta$. In the basis of the coupled modes $E_{1,2}(r)$, the Hamiltonian is given by:

$$\mathrm{H}' = \hbar \begin{bmatrix} \omega_0 & \alpha g & \beta g \\ \alpha g & \tilde{\omega}_1 & 0 \\ \beta g & 0 & \tilde{\omega}_2 \end{bmatrix}$$

where $\tilde{\omega}_{1,2} = \omega_{1,2} - i\kappa_{1,2}$ are the complex eigenvalues of the coupled modes. The effective dipole-coupled-mode interaction rates $g_1 = \alpha g$ and $g_2 = \beta g$ and the loss rates $\kappa_{1,2}$ are functions of the detuning between the two cavities and can be controlled by tuning one of them. The SE rate into one of the coupled modes, normalized by the SE rate in the unperturbed target cavity, is given by:

$$\frac{\gamma_1}{\gamma_t} \cong |\alpha|^2 \frac{\kappa_t}{\kappa_1} = |\alpha|^2 \frac{Q_1}{Q_t}$$

which shows that SE is affected both by the change in the coupling rate g (term $|\alpha|^2$) and loss rate κ. This simple model applies to a single, spectrally narrow emitter. As our experiments involve an ensemble of QDs with non-negligible homogeneous broadening, the Master equation, with the addition of the emitter's decoherence and incoherent pumping, has been used to reproduce the data in Figs 2 and 3. More details are provided in the Supplementary Information.

Sample preparation. The sample was grown on an InP(100) substrate by metal–organic vapour phase epitaxy. The structure contains a InP buffer layer of thickness 100 nm, followed by a 110 nm lattice-matched InGaAsP layer with a bandgap at 0.992 eV (Q1.25), a GaAs interlayer 1.2 monolayers thick, a single layer of InAs QDs, a 110 nm InGaAsP layer and a 50 nm InP capping layer. The QDs have an areal density of 2×10^9 cm^{-2} and provide a 100 nm broad luminescence peak around 1,550 nm (ref. 28), which feeds the cavity mode. The PhC cavities were fabricated with a standard process of electron-beam lithography and inductively coupled plasma using a $Cl_2/Ar/H_2$ mixture. The selective wet etching of the InP sacrificial layer was carried out in a HCl/H_2O solution at 2 °C. The lattice constant of PhC is chosen to be $\alpha_0 = 480$ nm with a filling factor of 0.30 to achieve a cavity mode around 1,550 nm at 77 K. The target and FP cavity consist of two and 80 periods of modulated lattice constant ($\alpha_1 = 1.03 \times \alpha_0$), respectively. The barrier between two cavities contains four periods of the original lattice constant.

Experimental set-up. The measurement was performed at 77 K using a confocal microscopy set-up in which two laser beams are focused at different positions with a separation of 30 μm, as indicated in the sketch in Fig. 1c. The temperature was chosen to facilitate the thermal tuning of the cavities. The μPL signal from the target cavity was collected by the objective and measured with a spectrometer. The experiments on thermo-optic tuning (Fig. 2) were performed by exciting the target cavity with a pulsed laser at 1,064 nm, pulse width of 6 ps and energy of 2 μJ cm^{-2} per pulse, with the FP cavity heated by a continuous wave (CW) beam at 780 nm. Decay curves at different detunings were measured by time-correlated single-photon counting (TCSPC) using a superconducting single-photon detector by filtering out the cavity peak with a narrow bandpass filter (FWHM = 0.5 nm)[29]. In the ultrafast tuning experiments (Fig. 3) the target cavity was pumped with the CW beam at 780 nm as the FP cavity was excited with the 1,064 nm pulsed laser of energy 200 μJ cm^{-2} per pulse, and the time-resolved PL from the target cavity was measured by TCSPC. In the dynamic modulation experiment of Fig. 4 both the target and the FP cavities were excited with the pulsed laser, at different delays, with energies of 20 and 200 μJ cm^{-2} per pulse, respectively. The fine adjustment of the wavelength detuning between two cavities was achieved by coupling a CW lasing beam at 780 nm on the FP cavity.

Received 11 February 2014; accepted 7 August 2014; published online 14 September 2014

References

1. Shields, A. J. Semiconductor quantum light sources. *Nature Photon* **1,** 215–223 (2007).
2. Raimond, J. M., Brune, M. & Haroche, S. Manipulating quantum entanglement with atoms and photons in a cavity. *Rev. Mod. Phys.* **73,** 565–582 (2001).
3. Cirac, J. I., Zoller, P., Kimble, H. J. & Mabuchi, H. Quantum state transfer and entanglement distribution among distant nodes in a quantum network. *Phys. Rev. Lett.* **78,** 3221–3224 (1997).
4. Parkins, A. S., Marte, P. & Zoller, P. Synthesis of arbitrary quantum states via adiabatic transfer of Zeeman coherence. *Phys. Rev. Lett.* **71,** 3095–3098 (1993).
5. Kuhn, A., Hennrich, M. & Rempe, G. Deterministic single-photon source for distributed quantum networking. *Phys. Rev. Lett.* **89,** 067901 (2002).
6. Yin, Y. *et al.* Catch and release of microwave photon states. *Phys. Rev. Lett.* **110,** 107001 (2013).
7. Faraon, A., Majumdar, A., Kim, H., Petroff, P. & Vučković, J. Fast electrical control of a quantum dot strongly coupled to a photonic-crystal cavity. *Phys. Rev. Lett.* **104,** 047402 (2010).
8. Trotta, R. *et al.* Nanomembrane quantum-light-emitting diodes integrated onto piezoelectric actuators. *Adv. Mater.* **24,** 2668–2672 (2012).

9. Fuhrmann, D. A. *et al.* Dynamic modulation of photonic crystal nanocavities using gigahertz acoustic phonons. *Nature Photon.* **5,** 605–609 (2011).
10. Midolo, L., van Veldhoven, P. J., Dündar, M. A., Nötzel, R. & Fiore, A. Electromechanical wavelength tuning of double-membrane photonic crystal cavities. *Appl. Phys. Lett.* **98,** 211120 (2011).
11. Johnson, P. M., Koenderink, A. F. & Vos, W. L. Ultrafast switching of photonic density of states in photonic crystals. *Phys. Rev. B* **66,** 081102 (2002).
12. Thyrrestrup, H., Hartsuiker, A., Gérard, J-M. & Vos, W. L. Non-exponential spontaneous emission dynamics for emitters in a time-dependent optical cavity. *Opt. Express* **21,** 23130 (2013).
13. Tanaka, Y. *et al.* Dynamic control of the Q-factor in a photonic crystal nanocavity. *Nature Mater.* **6,** 862–865 (2007).
14. Tanabe, T., Notomi, M., Taniyama, H. & Kuramochi, E. Dynamic release of trapped light from an ultrahigh-Q nanocavity via adiabatic frequency tuning. *Phys. Rev. Lett.* **102,** 043907 (2009).
15. Vignolini, S. *et al.* Near-field imaging of coupled photonic-crystal microcavities. *Appl. Phys. Lett.* **94,** 151103 (2009).
16. Intonti, F. *et al.* Young's type interference for probing the mode symmetry in photonic structures. *Phys. Rev. Lett.* **106,** 143901 (2011).
17. Sato, Y. *et al.* Strong coupling between distant photonic nanocavities and its dynamic control. *Nature Photon.* **6,** 56–61 (2011).
18. Notomi, M. *et al.* Nonlinear and adiabatic control of high-Q photonic crystal nanocavities. *Opt. Express* **15,** 17458–17481 (2007).
19. Hughes, S. Coupled-cavity QED using planar photonic crystals. *Phys. Rev. Lett.* **98,** 083603 (2007).
20. Song, B-S., Noda, S., Asano, T. & Akahane, Y. Ultra-high-Q photonic double-heterostructure nanocavity. *Nature Mater.* **4,** 207–210 (2005).
21. Dündar, M. A., Voorbraak, J. A. M., Nötzel, R., Fiore, A. & van der Heijden, R. W. Multimodal strong coupling of photonic crystal cavities of dissimilar size. *Appl. Phys. Lett.* **100,** 081107 (2009).
22. Fujita, M., Takahashi, S., Tanaka, Y., Asano, T. & Noda, S. Simultaneous inhibition and redistribution of spontaneous light emission in photonic crystals. *Science* **308,** 1296 (2005).
23. Fushman, I. *et al.* Ultrafast nonlinear optical tuning of photonic crystal cavities. *Appl. Phys. Lett.* **90,** 091118 (2007).
24. Johne, R. & Fiore, A. Single-photon absorption and dynamic control of the exciton energy in a coupled quantum-dot–cavity system. *Phys. Rev. A* **84,** 053850 (2011).
25. Fox, A. M., Miller, D. A. B., Livescu, G., Cunningham, J. E. & William, Y. J. Quantum well carrier sweep out: relation to electroabsorption and exciton saturation. *IEEE J. Quant. Electron.* **27,** 2281–2295 (1991).
26. Vasil'ev, P. P. Ultrashort pulse generation in diode lasers. *Opt. Quant. Electron.* **24,** 801–824 (1992).
27. Cohen-Tannoudji, C. Manipulating atoms with photons. *Phys. Scripta* **33,** T076 (1998).
28. Anantathanasarn, S., Nötzel, R., van Veldhoven, P. J., Eijkemans, T. J. & Wolter, J. H. Wavelength-tunable (1.55-μm region) InAs quantum dots in InGaAsP/InP (100) grown by metal–organic vapor-phase epitaxy. *J. Appl. Phys.* **99,** 013503 (2003).
29. Zinoni, C. *et al.* Single-photon experiments at telecommunication wavelengths using nanowire superconducting detectors. *Appl. Phys. Lett.* **91,** 031106 (2007).

Acknowledgements

The nanofabrication work was carried out in the NanoLab@TU/e cleanroom. The authors are grateful to B. Wang, M. A. Dündar and R. W. van der Heijden for fruitful discussions on the fabrication and experiments, to Z. Zhou, D. Sahin, F. M. Pagliano, C. P. Dietrich, E. J. Geluk, E. Smalbrugge, T. de Vries, M. van Vlokhoven, J. M. van Ruijven and P. A. M. Nouwens for technical support, to V. Savona for useful discussions on the theoretical aspects and to P. M. Koenraad and E. Pelucchi for a critical reading of the manuscript. This research is supported financially by NanoNextNL, a micro and nanotechnology program of the Dutch Ministry of Economic Affairs, Agriculture and Innovation (EL&I) and 130 partners, the Dutch Technology Foundation STW, Applied Science Division of NWO, the Technology Program of the Ministry of Economic Affairs under project No. 10380 and the FOM project No. 09PR2675. One of the authors (A.F.) dedicates this work to the memory of E. Rosencher.

Author contributions

A.F. proposed the experiment and led the project. C-Y.J., M.Y.S. and L.M. performed the optical simulations. P.J.V. grew the sample. C-Y.J. designed and fabricated the devices. C-Y.J., M.Y.S. and T.B.H. performed the measurements. R.J. developed the theory. C-Y.J., R.J., A.F. and L.M. prepared the manuscript. All authors contributed to the discussion.

Additional information

Supplementary information is available in the online version of the paper. Reprints and permissions information is available online at www.nature.com/reprints. Correspondence and requests for materials should be addressed to C-Y.J.

Competing financial interests

The authors declare no competing financial interests.